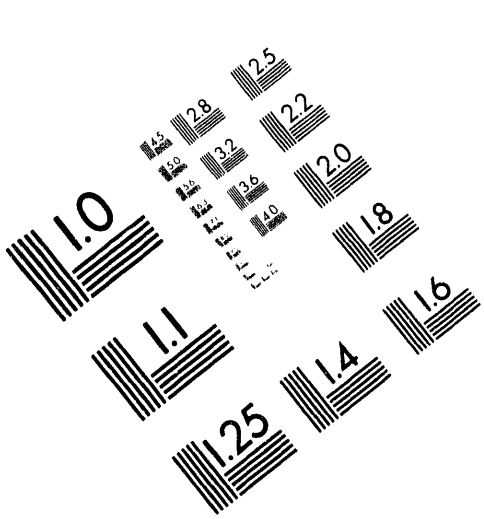

Association for Information and Image Management

1100 Wayne Avenue, Suite 1100
Silver Spring, Maryland 20910
301/587-8202

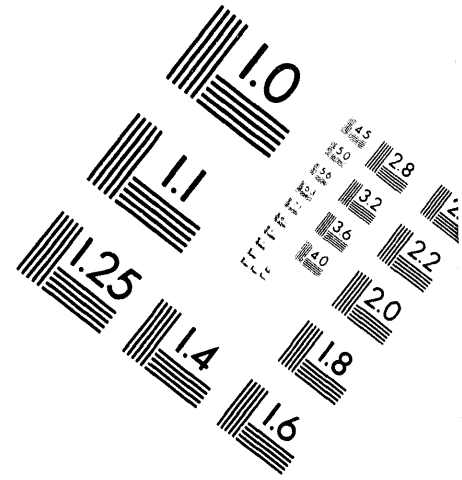

Centimeter

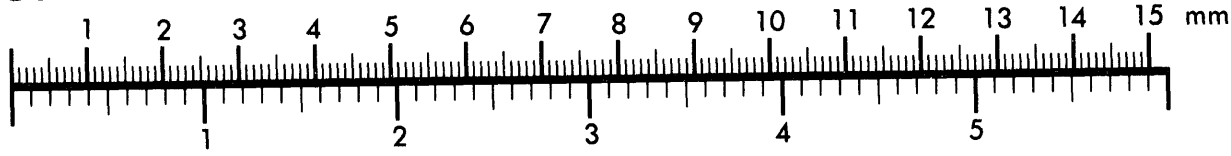

Inches

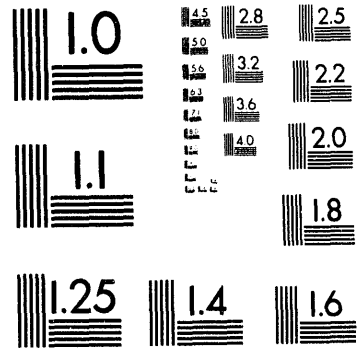

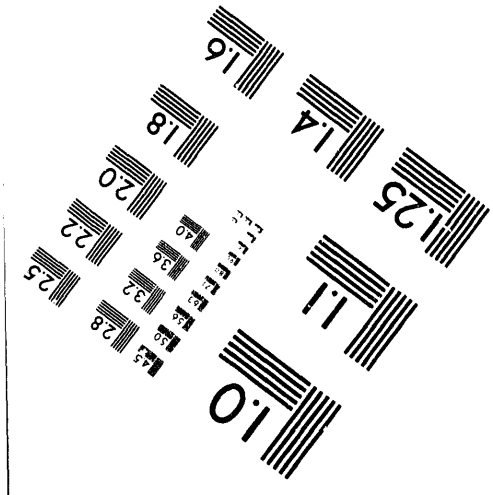

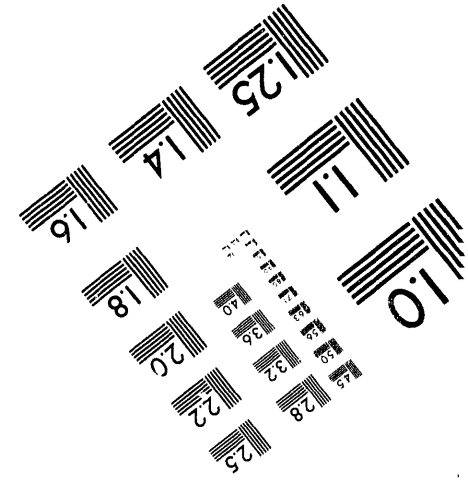

MANUFACTURED TO AIIM STANDARDS
BY APPLIED IMAGE, INC.

1 of 1

CONF-940286--4

ON THE CRACK GROWTH RESISTANCE AND STRENGTH OF THE B2 IRON ALUMINIDES Fe-40Al, Fe-45Al, AND Fe-10Ni-40Al (at. %)

J. H. Schneibel and P. J. Maziasz

Oak Ridge National Laboratory
Metals and Ceramics Division
P. O. Box 2008
Oak Ridge, TN 37831-6114

Abstract

The crack growth resistance and yield strength of the B2 iron aluminides Fe-40Al, Fe-45Al, and Fe-10Ni-40Al (at. %) have been investigated at room temperature in laboratory air. After fast cooling from 1273 K, Fe-45Al and Fe-10Ni-40Al are much stronger than Fe-40Al and exhibit considerably lower crack growth resistance. The crack growth resistance decreases with decreasing crack propagation velocity. Low crack propagation velocities favor intergranular fracture, whereas high velocities can lead to significant contributions from transgranular fracture. Boron additions to Fe-40Al and Fe-10Ni-40Al improve the crack growth resistance, reduce its dependence on the crack propagation velocity, and cause the fracture path to be predominantly transgranular. In a plot of fracture toughness versus yield strength, the properties of the iron aluminides are similar to those of typical aluminum alloys.

Introduction

Like many intermetallics, iron aluminides suffer from low room-temperature ductility and fracture toughness. One important reason for the low ductility of iron aluminides is the humidity induced hydrogen embrittlement first identified in these materials by Liu et al. (1) and substantiated by subsequent work (2-4). It is thought that aluminum atoms, which are freshly exposed during a tensile test, are oxidized by water vapor contained in the surrounding air. The oxidation is accompanied by a release of atomic hydrogen, which in turn causes hydrogen embrittlement. In addition to this environmental effect, the ductility and fracture toughness of iron aluminides are also likely to depend on their strength, which in turn is known to depend strongly on the heat treatment (5,6) and may also depend strongly on alloying additions (7). Another point of interest is the fracture mode. Whether transgranular (TG) or intergranular (IG) fracture occurs depends, as we shall see, on a variety of circumstances such as crack propagation velocity and micro- or macroalloying additions. Owing to the humidity induced embrittlement, we also expect kinetic effects, i.e., a dependence of the crack growth resistance on the crack propagation velocity. At very high rates, for example, the oxidation of aluminum by water vapor may not occur fast enough to cause embrittlement, whereas low rates would provide enough time to favor embrittlement. In order to obtain more information on these kinetic effects, we chose controlled fracture experiments, in which the crack velocity and therefore the rate with which fresh aluminum atoms are exposed at the crack tip, can be varied over a wide range. As an example of a microalloying effect, we studied the influence of boron, which is known to segregate to the grain boundaries (GBs) and to enhance the GB strength (2). An example of macroalloying is provided by Ni, which is soluble in FeAl and increases its strength significantly (7,8). All alloys investigated in this work exhibit the B2 (CsCl) structure.

Experimental Procedure

Several iron aluminide alloys were arc-cast in argon from elemental constituents with typical purities of 99.9 wt %. A chemical analysis of Fe-40 at. % Al is provided in Table I. Note that compositions are assumed to be in at. % unless otherwise noted.

Table I Chemical Analysis of an Alloy with the Nominal Composition Fe-40 at. % Al

	Fe	Al	C	S	Si	Cr	Mo	Nb	Zr	N	O
wt %	75.8	24.1	0.029	0.001	0.01	<0.01	<0.01	<0.01	<0.01	0.004	0.009
at. % *	60.24	39.65	0.11								

* Considering only Fe, Al, and C.

The castings, which had diameters and lengths of 25 and 120 mm, respectively, were extruded in mild steel cans at 1173 K with an area reduction of 9:1. Chevron-notched bend specimens with cross sections of approximately 5 by 5 mm and lengths of 45 mm were prepared by electro-discharge machining (EDM) and grinding. These specimens, which are schematically shown in Figure 1, were annealed for 1 h at 1273 K in vacuum, fast cooled in the cold zone of the vacuum system, and then tested in a universal testing machine in 3-point bending (40-mm span) in laboratory air [typical relative humidity (RH) ranging from 20 to 80%] at room temperature. Some specimens were annealed for 1 week at 673 K in air prior to testing. The pupose of this anneal was to eliminate thermal vacancies which might have been quenched in during the fast cooling from 1273 K (5).

Specimens were tested at different crosshead speeds, and load-load point displacement curves were obtained. For the particular geometry chosen, the crack velocity is roughly one-tenth of the crosshead speed. The stress intensity factors (SIFs) needed to drive the cracks were evaluated according to a procedure described in earlier papers (9,10). Since this procedure is somewhat involved, it should be pointed out that a reasonable value for the SIF may also be obtained by integrating the whole load-point displacement curve (an energy) and dividing it by the created

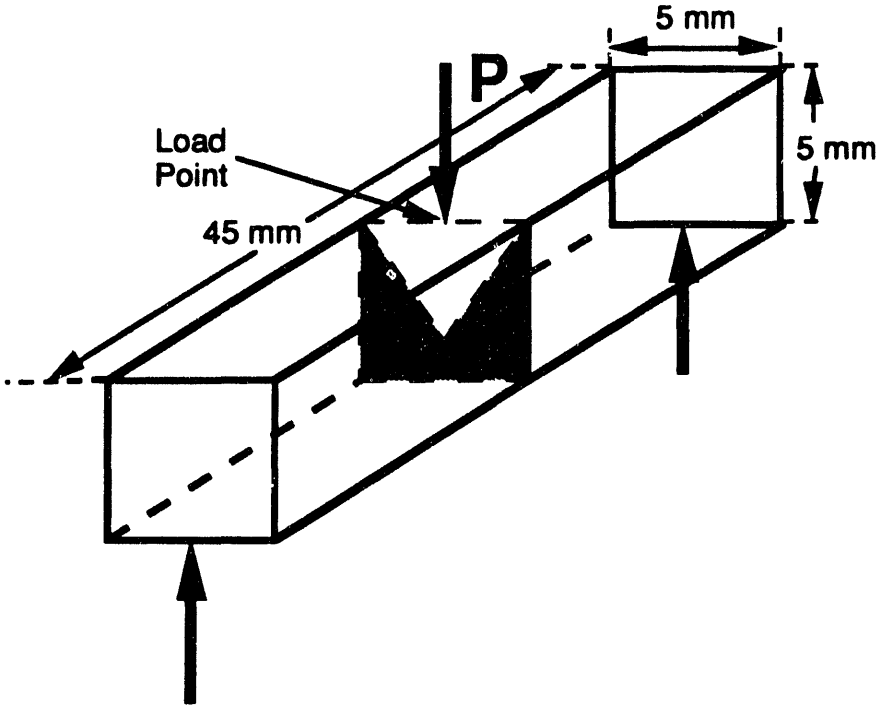

Figure 1 - Schematic of chevron-notched specimen for three-point bending.

surface area. The SIF is then given by this surface work of fracture (WOF) and the plane-strain Young's modulus E' as:

$$K_I = (2\ WOF\ E')^{1/2}. \qquad (1)$$

A value of 180 GPa was assumed for E' (9). For clarification, it should be noted that the WOF is often defined as the energy needed to break the specimen divided by the area swept out by the advancing crack. In this case, the factor two in Eq. (1) would be omitted. Since the samples are relatively small, the conditions for plane-strain fracture may not be fulfilled. However, since the sample geometry was always kept the same, the results obtained for the different alloys may be compared.

Small compression specimens (diameter typically 2.5 mm, height 5 mm) were machined by EDM from broken chevron-notch specimens. They were tested at room temperature at a crosshead speed resulting in an initial strain rate of 10^{-3} s^{-1}. A 0.2% yield stress was evaluated from the load-displacement curves obtained.

Two directionally solidified (DS) Fe-40Al ingots were produced in tapered alumina crucibles (diameter approximately 10 mm, length approximately 60 mm) in a Bridgman-type furnace. Processing was carried out in argon at 1773 K, and the withdrawal rate was 25 mm/h.

The fracture surfaces of the tested chevron-notch specimens were examined in a scanning electron microscope (SEM) in order to assess whether the fracture mode was IG or TG. Attention was focused on the area within approximately 2 mm of the chevron tip.

Experimental Results and Discussion

Crack Growth Resistance

Figure 2 shows the SIF, or crack growth resistance, for Fe-40Al and Fe-40Al-0.1B (10). The decrease in the SIF of Fe-40Al with decreasing crack velocity is accompanied by a transition from mixed IG-TG fracture to complete IG fracture as shown in Figure 3. This suggests that the humidity induced embrittlement occurs preferentially at the GBs and that the embrittlement of the GBs is particularly severe when enough time is available. The grain sizes in the boron-free and the boron-doped Fe-40Al are comparable (Table II). However, the Fe-40Al without boron contains stringers of fine grains. When boron is added, the fracture mode becomes completely

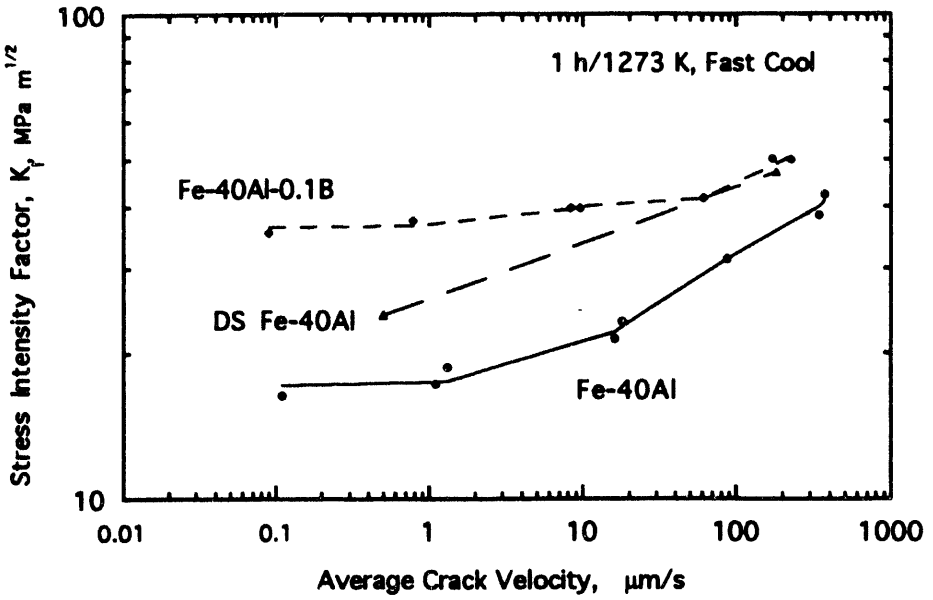

Figure 2 - Crack growth resistances of polycrystalline and directionally solidified iron aluminides for different crack velocities.

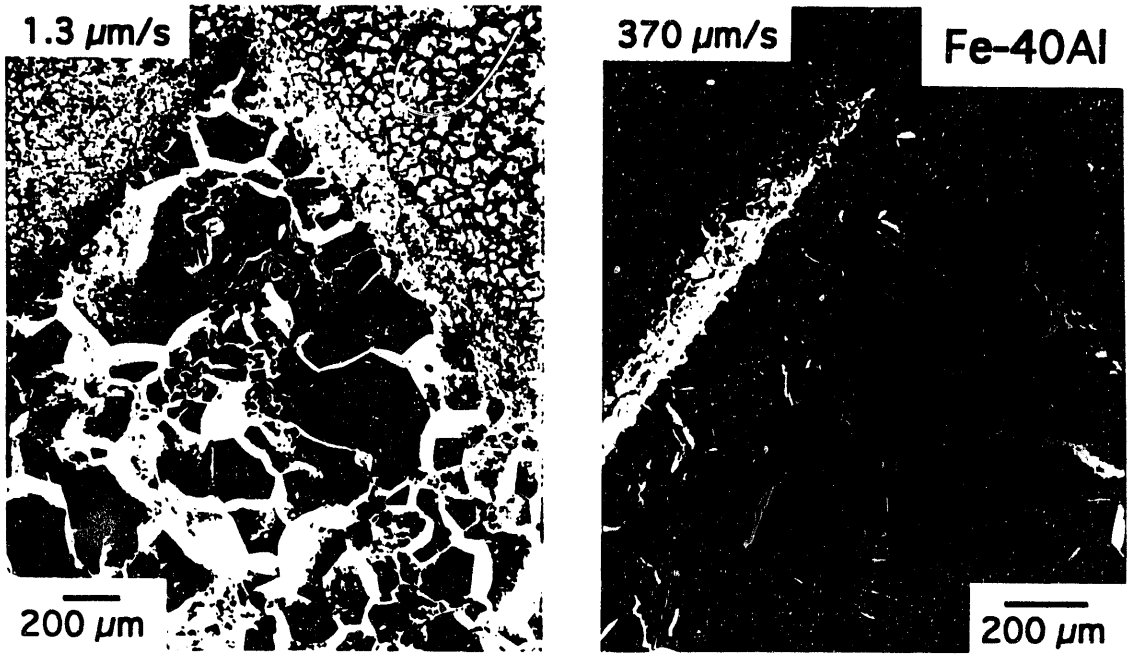

Figure 3 - Fracture surfaces of Fe-40Al for low and high crack velocities.

Table II Grain Sizes (Mean Linear Intercept Length) of Iron Aluminides after Extrusion and Annealing for 1h at 1273 K

Composition (at.%)	Mean Linear Intercept Length (μm)
Fe-40Al	209*
Fe-40Al-0.1B	147
Fe-10Ni-40Al	107
Fe-10Ni-40Al-0.1B	42

*The stringers of fine grains occuring in this alloy have been ignored.

TG and the SIF becomes almost independent of the crack velocity. This does not necessarily mean that humidity induced embrittlement is absent. If it is present, it is, however, not sensitive to the crack velocity, within the experimental window available.

As expected, the DS Fe-40Al material with its lack of transverse GBs exhibits higher SIFs than the extruded, polycrystalline material with the same nominal composition (Figure 2). However, the SIF at the lower crack velocity is well below the corresponding values for Fe-40Al-0.1B. This is presumably due to different orientations of the two DS specimens. Whereas the specimen with the higher SIF exhibited distinct 90° steps corresponding to {100} cleavage observed in FeAl (11), as well as cracks perpendicular to the crack path, the other specimen exhibited a fairly smooth fracture surface suggesting a low SIF (Figure 4).

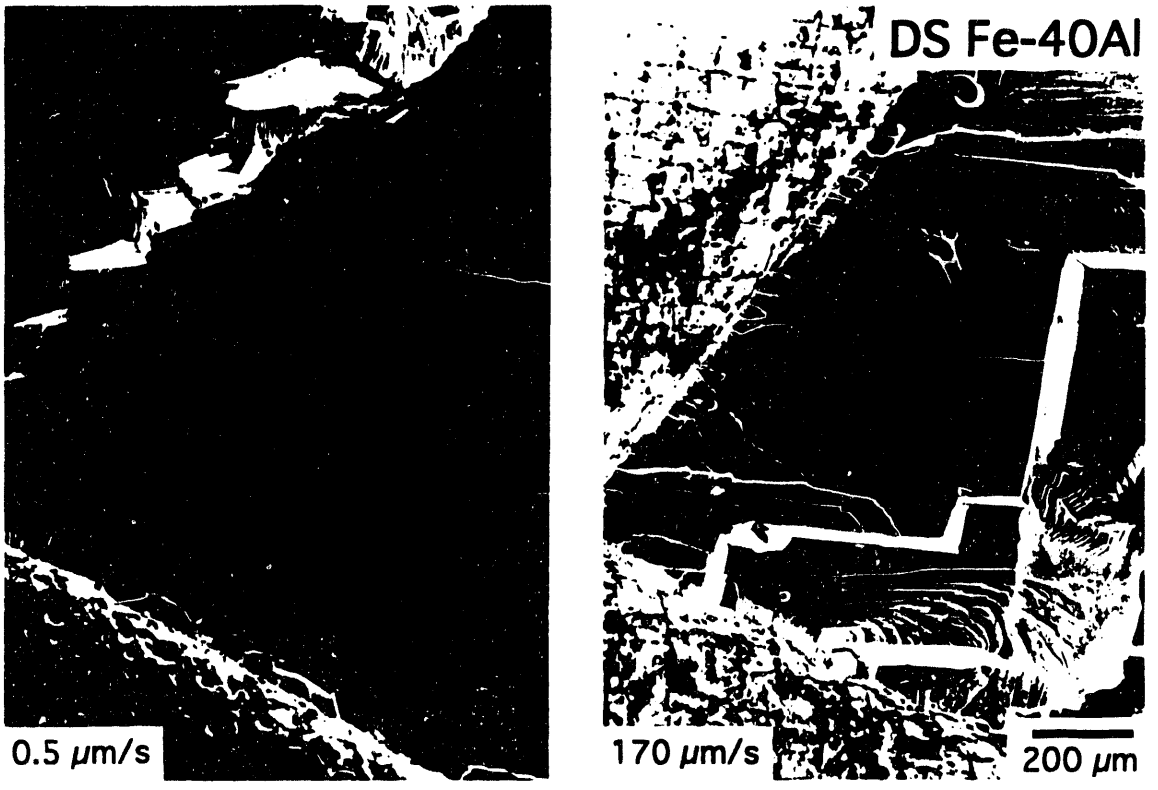

Figure 4 - Fracture surfaces of the two directionally solidified Fe-40Al specimens fractured with different average crack velocities. The magnifications in both pictures are the same.

It is well known that the ductility of FeAl decreases and that the propensity for IG fracture increases as the aluminum concentration increases (12). Figure 5 shows accordingly that the SIFs for Fe-45Al are much lower than those for Fe-40Al. Annealing for 1 week at 673 K, in addition to 1 hour at 673 K, increases the crack growth resistance somewhat. Fracture in Fe-45Al occured intergranularly regardless of the annealing treatment.

The SIFs for Fe-10Ni-40Al and Fe-10Ni-40Al-0.1B, shown in Figure 6, are similar to those of Fe-45Al. The SIF of Fe-10Ni-40Al increases only slightly as the crack velocity increases. This small increase is accompanied by a transition from mostly IG to mostly TG fracture, indicating that these two fracture paths have a very similar crack growth resistance (Figure 7). Thus, the fracture behavior of Fe-10Ni-40Al is qualitatively similar to that of Fe-40Al with the main difference being that the SIFs are much lower. Again, when boron is added, the fracture mode becomes TG over the whole range of crack velocities.

The mechanism proposed for humidity induced hydrogen embrittlement, as it stands now, is very general. It is based on the reduction of water vapor by the oxidation of aluminum, and it does not contain any other assumptions such as crystal structure and the effect of other alloying additions. It seems, therefore, justified to compare the slow crack growth of iron aluminides to

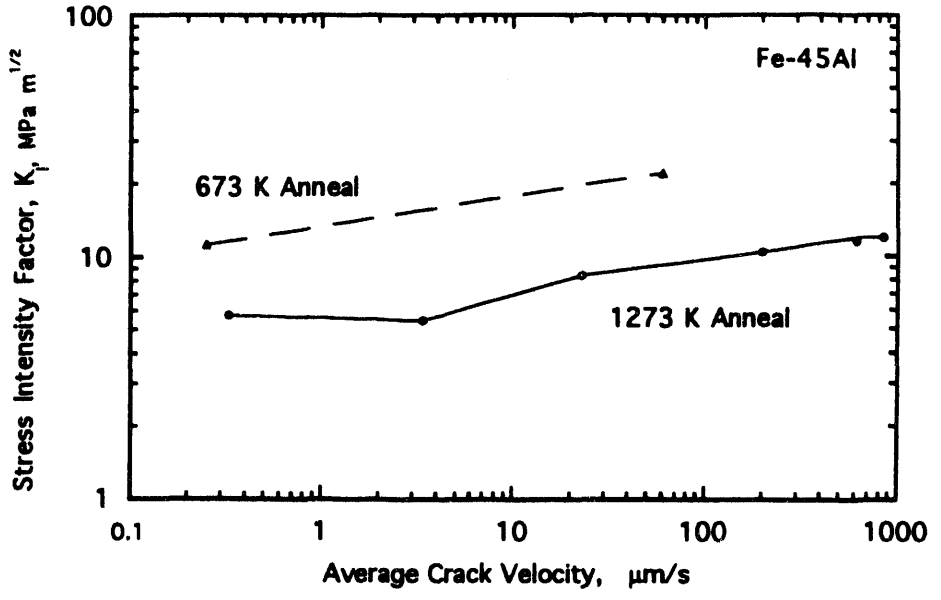

Figure 5 - Crack growth resistances of Fe-45Al for different crack velocities and annealing treatments.

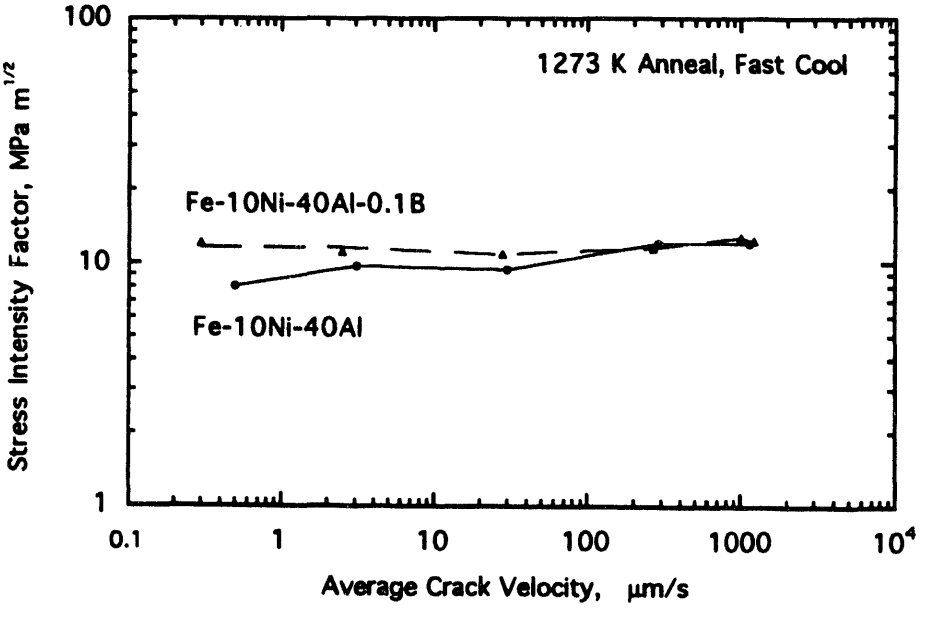

Figure 6. - Crack growth resistances of Fe-10Ni-40Al and Fe-10Ni-40Al-0.1B for different crack velocities.

that of aluminum alloys. This has been done in Figure 8 using our data for Fe-40Al and published data for the AlZnMg aluminum alloys 7179-T651 and 7075-T651 (13,14). It is seen that the aluminum alloys and FeAl behave in a qualitatively similar manner, although the humidity embrittlement of aluminium alloys tends to occur at lower crack velocities. It should also be noted that in the aluminum alloys other elements such as Mg are likely to be involved in the stress corrosion process. The data in Figure 8 indicates also that the threshold SIF for

Fe-40Al is higher than that for the aluminum alloys, although more measurements at lower crack velocities will be required in order to confirm this.

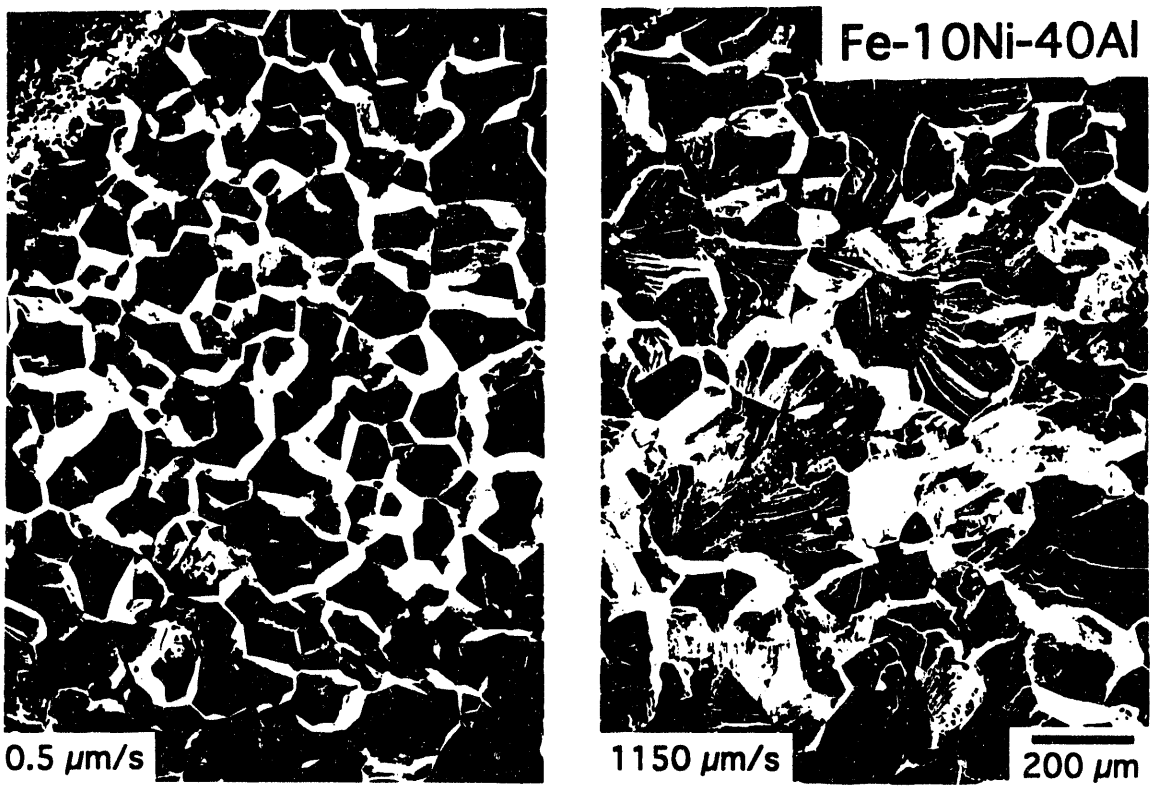

Figure 7. - Fracture surfaces of Fe-10Ni-40Al for two different crack velocities. Both micrographs have the same magnification.

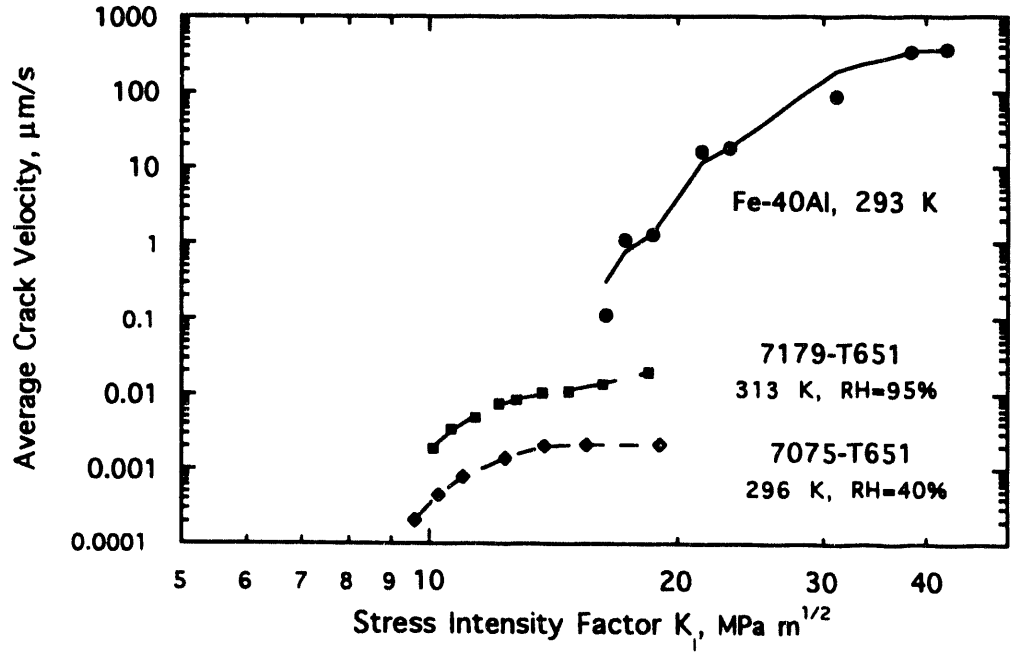

Figure 8. - Comparison of slow crack growth in Fe-40Al and two aluminum alloys.

Compressive Strength

The results of the compression tests are summarized in Table III. Several points are worth mentioning. After fast cooling from 1273 K, the yield strength of boron-doped Fe-40Al is lower than that of undoped Fe-40Al. This may indicate that boron interacts with the thermal vacancies in Fe-40Al and reduces their concentration. If Fe-40Al and Fe-40Al-0.1B are additionally annealed for 1 week at 673 K, this relationship reverses—the boron-doped material is slightly stronger than the undoped one. This suggests that boron causes a small amount of solid solution strengthening [or precipitation strengthening, if very fine borides form as in NiAl (15)].

Table III Compressive Yield Strengths (MPa) for Different Iron Aluminide Compositions and Heat Treatments

Composition (at. %)	1 h/1273 K Fast Cool	Average Values and Standard Deviations	1 h/1273 K/Fast Cool + 1week/673 K/air	Average Values and Standard Deviations
Fe40Al	578	584 ± 8	291	300 ± 7
Fe40Al	590		303	
Fe40Al			299	
Fe40Al			306	
Fe40Al0.1B	460	451 ± 13	333	331 ± 9
Fe40Al0.1B	442		338	
Fe40Al0.1B			321	
Fe45Al	924	916 ± 8	239	224 ± 11
Fe45Al	908		215	
Fe45Al	917		220	
Fe45Al			221	
Fe10Ni40Al	850	850	852	848 ± 5
Fe10Ni40Al	850		849	
Fe10Ni40Al			842	
Fe10Ni40Al0.1B	860	858 ± 4	841	844 ± 4
Fe10Ni40Al0.1B	855		846	

In agreement with a large body of work [see for example (6)], the strength of Fe-45Al annealed at a high temperature (e.g., 1273 K) and cooled quickly is very high and decreases substantially after a long-term, low-temperature anneal. This is due to the removal of thermal point defects, in particular vacancies, quenched in during cooling from high temperatures An additional point, the reasons for which are not clear, is that Fe-45Al annealed at a low temperature is significantly softer than Fe-40Al heat-treated in the same way.

When Ni is added, the situation is quite different. The strength of Fe-10Ni-40Al is practically unaffected by 0.1 at. % B. An anneal for 1 week at 673 K does not reduce its yield strength substantially. This result is in qualitative agreement with Kong and Munroe's (7) hardness measurements on (Fe, Ni)Al intermetallics. These authors noted that the high hardness of FeAl containing even small amounts of Ni cannot be removed by low-temperature anneals. The exact reasons for this finding are not clear. The nickel addition may cause such strong solid solution strengthening that any thermal vacancy contributions may not be readily detectable (note that solution strengthening varies as the square root of the concentration), or the Ni may in some way reduce the thermal defect concentration.

Yield Strength, Crack Growth Resistance, and Fracture Mode

Figure 9 compares the SIFs measured for the investigated iron aluminides (at crack velocities on the order of 1 μm/s) to the plane strain fracture toughnesses of Al alloys (16), as a function of yield strength. As usual, an inverse relationship is observed. Interestingly, the SIFs of the iron aluminides are comparable to those for the aluminum alloys, and in that sense, iron aluminides are not particularly brittle. In the iron aluminides, the SIFs for IG and TG fracture tend to lie

close together. This is particularly true in the Fe-10Ni-40Al alloys. If the aluminum content is raised to 45 at. %, the fracture path is always IG. One interesting point to note is that the dramatic reduction of the yield strength of Fe-45Al after low-temperature annealing is not accompanied by a substantial increase in the crack growth resistance. This suggests that yield strength reductions in themselves do not necessarily result in high fracture toughnesses, if a weak fracture path is available. Therefore, an adequate GB strength is necessary. This may be achieved by reducing the aluminum content, or by adding GB strengtheners such as boron.

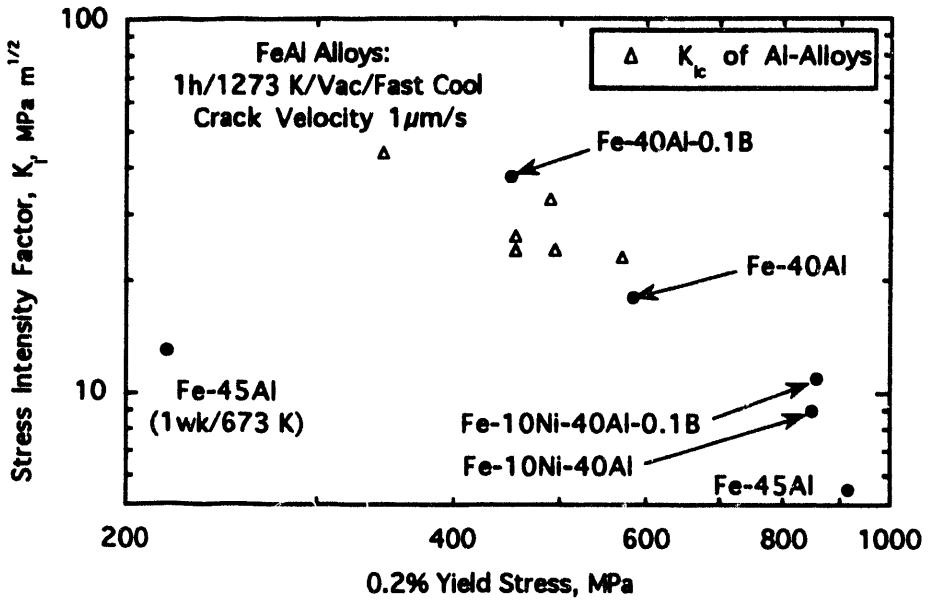

Figure 9 - Comparison of the crack growth resistances of FeAl and aluminum alloys.

Conclusions

1. The crack growth resistance and yield strength of B2 iron aluminides can be significantly influenced by stoichiometry, alloying additions, and heat treatment.
2. Alloying of Fe-40Al with Ni removes the sensitivity of its yield strength to heat treatment.
3. High crack velocities encourage TG fracture, whereas low velocities favor IG fracture. In Fe-10Ni40Al, the SIFs required for IG or TG fracture are almost identical.
4. Iron aluminide alloys containing 40 at. % Al show crack growth resistances which are similar to those of aluminum alloys with comparable yield strengths.
5. The example of Fe-45Al shows that a pronounced reduction in yield strength is not necessarily accompanied by a strong increase in the crack growth resistance, if a weak fracture path is available.

Acknowledgments

The authors would like to thank D. J. Alexander and C. G. McKamey for their review of this paper. Thanks also go to K. Spence for editing. This research was sponsored by the Division of Materials Sciences, U.S. Department of Energy, under contract DE-AC05-84OR214000 with Martin Marietta Energy Systems, Inc.

References

1. C. T. Liu, E. H. Lee, and C. G. McKamey, Scr. Metall., 23 (1989), 875.

2. C. T. Liu and E. P. George, Scr. Metall. Mater., 24 (1990), 1285 .

3. R. J. Lynch, L. A. Heldt, and W. W. Milligan, Scr. Metall. Mater., 25 (1991), 2147.

4. C. T. Liu, C. G. McKamey, and E. H. Lee, Scr. Metall. Mater., 24 (1990), 385.

5. P. Nagpal and I. Baker, Metall. Trans. A, 21A (1990), 2281.

6. Y. A. Chang, L. M. Pike, C. T. Liu, A. R. Bilbrey, and D. S. Stone, Intermetallics, 1 (1993), 107.

7. C. H. Kong and P. R. Munroe, Scr. Metall. Mater., 28 (1993), 1241.

8. I. Jung, M. Rudy, and G. Sauthoff, High-Temperature Ordered Intermetallic Alloys II, vol. 81, eds. N. A. Stoloff, C. C. Koch, C. T. Liu, and O. Izumi (Pittsburgh, PA: Materials Research Society, 1993), 263-274.

9. J. H. Schneibel and M. G. Jenkins, Scr. Metall. Mater., 28 (1993), 389.

10. J. H. Schneibel, M. G. Jenkins, and P. J. Maziasz, High-Temperature Ordered Intermetallic Alloys V, vol. 288, eds. I. Baker, R. Darolia, J. D. Whittenberger, and M. H. Yoo (Pittsburgh, PA: Materials Research Society, 1993), 549-554.

11. K.-M. Chang, R. Darolia, and H. A. Lipsitt, Acta Metall. Mater., 40 (1992), 2727.

12. I. Baker and D. J. Gaydosh, Mater. Sci. Engng., 96 (1987), 147.

13. G. M. Scamans, Hydrogen Effects in Metals, ed. I. M. Bernstein and A. W. Thompson (Moran, WY: The Metallurgical Soc. of AIME, 1981), 467-475.

14. R. W. Hertzberg, Deformation and Fracture Mechanics of Engineering Materials, (New York, NY: John Wiley & Sons, 1976).

15. R. Jayaram and M. K. Miller, Surf. Sci., 266 (1992), 310.

16. Metals Handbook, vol. 2 (Materials Park, OH: ASM International, 1990).

DATE
FILMED
10/19/94
END